atmosphere

MDPI

Article

Spatio-Temporal Characteristics in the Clearness Index Derived from Global Solar Radiation Observations in Korea

Yeonjin Jung [1], Hana Lee [1], Jaemin Kim [2], Youngbum Cho [3], Jhoon Kim [1] and Yun Gon Lee [2,*]

[1] Department of Atmospheric Sciences, Yonsei University, Seoul 03722, Korea; clover529@yonsei.ac.kr (Y.J.); leehn88@yonsei.ac.kr (H.L.); jkim2@yonsei.ac.kr (J.K.)

[2] Department of Atmospheric Sciences/Research Institute of Basic Sciences, Chungnam National University, Daejeon 34134, Korea; jaemin2984@gmail.com

[3] Department of Physics, University of Colorado, Boulder, CO 80309, USA; skyclub3@gmail.com

* Correspondence: yungonlee@gmail.com; Tel.: +82-42-821-6115

Academic Editor: Robert W. Talbot

Received: 8 March 2016; Accepted: 6 April 2016; Published: 12 April 2016

Abstract: The spatio-temporal characteristics of the clearness index (K_T) were investigated using daily global solar irradiance measurements (290–2800 nm) for the period of 2000–2014 at 21 sites in Korea, a complex region in East Asia with a distinct monsoon season and heavy aerosol loading year-round. The annual mean K_T value for all sites is 0.46, with values of 0.63 and 0.25 for clear and overcast skies, respectively. The seasonal variations in monthly average K_T show a minimum of 0.37 in July at all sites except for Jeju, where the value was 0.29 in January. The maximum value (K_T = 0.51) is observed in October, followed by a secondary peak (K_T = 0.49) during February–April. The lowest K_T value (K_T = 0.42) was observed at both the Seoul and Jeju sites, and the highest (K_T = 0.48) in the southeastern regions. Increases in average K_T exceeding 4% per decade were observed in the middle and southeastern regions, with the maximum (+8% per decade) at the Daegu site. Decreasing trends (<−4% per decade) were observed in the southwestern regions, with the maximum (−7% per decade) at the Mokpo site. Cloud amount, relative humidity, and aerosol optical depth together explained 57% of the variance in daily mean K_T values. The contributions of these three variables to variations in K_T are 42%, 9% and 6%, respectively. Thus, the variations in K_T in Korea can be primarily attributed to the presence of clouds and water vapor, with relatively weak aerosol effects.

Keywords: global solar radiation; clearness index; long-term trend; cloud; water vapor; aerosol; Korea

1. Introduction

Solar radiation in the ultraviolet, visible, and near-infrared ranges is the major source of energy for the climate and ecosystems on Earth. Global solar radiation refers to the total amount of solar energy reaching the Earth's surface, which varies dramatically over temporal and spatial scales due to varying atmospheric conditions above the surface. These variations can be attributed to the absorption and scattering of radiation by clouds, water vapor, aerosols, and other gases in the atmosphere, but are difficult to predict, primarily because of non-linear interactions in this complex system [1–3].

To quantify the extinction of solar radiation in the atmosphere, the combined contributions of various atmospheric parameters that affect incoming solar radiation need to be examined. While these extinction processes are complex, the estimation of sky conditions using incident solar radiation at a given location has been proposed as a simple approach. The ratio of the global solar radiation measured at the surface to the extraterrestrial solar radiation is defined as the clearness index (K_T) [4–8]. The clearness index has been used as a general indicator of the combined effects of the various extinction processes, which determine the transmission of solar radiation through the atmosphere.

There have been many studies characterizing sky conditions and long-term trends of solar radiation using K_T for a particular location [1,2,4,8,9]. The sky conditions at tropical stations in Nigeria were analyzed by the diurnal and seasonal variations of hourly and daily K_T [2,8]. Based on the 40 years (1961–2000) of daily solar radiation and monthly sunshine duration from China, the significant decreasing trends in K_T and global/direct radiation but increasing trend in diffuse radiation were evaluated [1]. Another approach is to develop empirical models for different wavelengths of radiation using sky conditions (*i.e.*, K_T) determined from the more commonly measured global solar radiation. These include models for ultraviolet radiation [10–15], erythemal ultraviolet radiation [16–19], photosynthetically active radiation (PAR) [20–22], and near-infrared radiation [23]. Using these models, the effects of several atmospheric parameters on the transmission of solar radiation have been assessed, including cloud cover [14,16,24,25], the presence of aerosols [9,26,27], and ozone concentration [12,19]. Additionally, studies of solar energy utilization systems and renewable energy have been performed in which regional K_T values were examined to determine the level of solar radiation availability [28,29].

Large variations in K_T occur on both temporal and spatial scales. The regional features of K_T and the effects of atmospheric parameters on K_T have not been sufficiently investigated over the Korean Peninsula where complex interactions of clouds, aerosols, and pollutants occur throughout the year, which includes a distinct monsoon season. Thus, the objective of this study is to evaluate spatio-temporal patterns in K_T over a recent time period together with long-term trends in K_T in Korea. Using a multiple regression model for K_T, we also estimate the individual contributions of several atmospheric parameters influencing K_T [30].

The remainder of this paper is organized as follows. Section 2 describes the data and methodology, and Sections 3.1 and 3.2 present information on temporal and spatial variations in K_T, respectively. Section 3.3 analyzes long-term trends in K_T and Section 3.4 investigates the individual contributions of atmospheric parameters to K_T variations. Finally, a summary and conclusions are given in Section 4.

2. Data and Methodology

The Korean Meteorological Administration (KMA) maintains 21 solar radiation measurement stations (Figure 1). The Gangneung site was established in January 2008, later than other sites. The KMA database provides hourly broadband global solar irradiance measurements. In this study, the daily irradiance data are used together with corresponding meteorological parameters measured at synoptic stations maintained by KMA over 15 years from January 2000 to December 2014 for all but one site (Gangneung). These sites are part of the World Meteorological Organization (WMO) network.

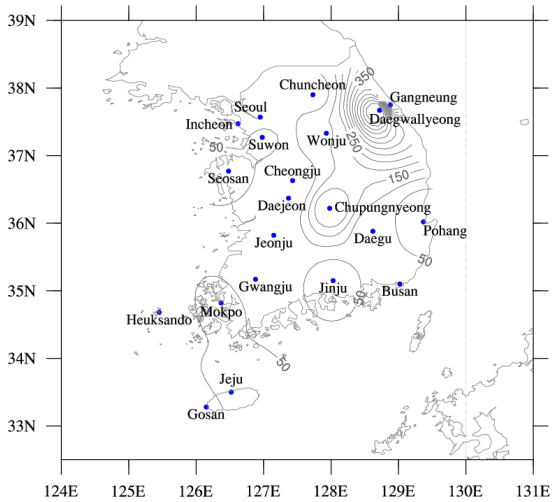

Figure 1. Spatial distribution of the global solar radiation network in Korea. An isoline contour at 50-m intervals represents the elevation.

2.1. Instruments and Data

Global solar irradiance (GS, 290–2800 nm) was measured using a pyranometer (CMP-21, Kipp & Zonen, Delft, Netherlands) with an experimental error of 3%. The CMP-21 pyranometer has a non-linearity below 0.2% in the range of 100–1000 Wm^{-2}, a directional response below 10 Wm^{-2} (up to 80° with a 1000 Wm^{-2} beam), and a temperature dependence below 1% (from −20 °C to 50 °C). The data were recorded as 1-minute average values using data loggers (CR21X, Campbell Scientific, Logan, UT, USA) and archived as hourly integrated values. The daily integrated values are the summation of 24 hourly measurements in units of Wm^{-2}. In addition, meteorological variables such as Cloud Amount (CA), Relative Humidity (RH), and Aerosol Optical Depth (AOD) were used. The CA is observed visually by KMA and expressed as tenths of the sky covered by clouds according to WMO standards. The RH is measured by Automated Weather Stations (AWS) installed at respective stations. The daily CA and RH are calculated by averaging eight values per day (03:00–24:00 LST). These instruments were installed after proper calibration, certified from the manufacturer, and have been recalibrated regularly. Because the ground-based measurements of AOD were limited, AOD at 550 nm was obtained from the Moderate Resolution Imaging Spectroradiometer (MODIS) Terra Collection 5.1 for the period of March 2000–December 2014. Thus, the long-term trend in AOD from March 2000 was analyzed and a regression model for K_T and meteorological variables was developed for the period covered by the AOD dataset.

2.2. Quality Assessment of Sample Data

The quality assessment of GS was based on two main criteria [31]. First, the observed surface GS should be less than the extraterrestrial GS in the same geographical area. Second, the observed surface GS should be larger than the minimum GS value under continuously overcast conditions. These criteria were used to identify outliers, which were removed from the data set. The K_T values and their anomalies were then calculated. Less than 1% of all measurement data were eliminated by the quality assessment process. Routine maintenance and control work were performed on-site daily, reducing the number of outlying data points.

2.3. Clearness Index

K_T is useful in characterizing the atmospheric transmission of radiation [4,5], and is defined as

$$K_T = \frac{H}{H_0} \tag{1}$$

where H is the global solar radiation measured on the horizontal surface and H_0 is the extraterrestrial solar radiation. K_T has also been expressed as the total solar transmissivity for UV-B [32] and PAR [33,34] attenuation, respectively.

Daily extraterrestrial solar radiation at the top of atmosphere, H_0, is calculated as follows [5]:

$$H_0 = \frac{24}{\pi} I_{sc} E_0 [\left(\frac{\pi}{180}\right) \omega_s \left(\sin\delta\sin\phi\right) + \left(\cos\delta\cos\phi\sin\omega_s\right)] \tag{2}$$

where I_{sc} is the solar constant (1367 Wm^{-2}), E_0 is the eccentricity correction factor of the Earth's orbit, ϕ is the latitude, δ is the solar declination angle, and ω_s is the sunrise hour angle. E_0 is given by Duffie and Beckman [35] as follows:

$$E_0 = 1 + 0.033\cos[\frac{360}{365}\left(d_n + 284\right)] \tag{3}$$

where d_n is the day of year. The term δ is calculated as follows [36]:

$$\delta = 23.45\sin[\frac{360}{365}\left(d_n + 284\right)] \tag{4}$$

We also conducted multiple linear regressions and analyzed partial correlation coefficients in order to estimate the individual contributions of the parameters influencing K_T [30].

3. Results and Discussion

3.1. Temporal Variations

Figure 2 shows temporal variations in monthly mean K_T values under three sky conditions (*i.e.*, all, clear (fractional cloud cover values, $N < 0.3$), and overcast ($N > 0.7$) skies), averaged over the 21 sites for the period of 2000–2014. The monthly mean K_T values under all-sky conditions at each site are summarized in Table 1. When averaged over all sites, the annual mean value of K_T under all-sky conditions was 0.46, as shown in Figure 2 and Table 1. The monthly values show a maximum of 0.51 in October and a secondary maximum of 0.49 in February, March, and April. A minimum of 0.37 in July and secondary minimum of 0.41 in August are observed. Overall, there are higher values during autumn, winter, and spring, and lower values in the summer. Monthly variations in the meteorological variables (*i.e.*, CA, RH, and AOD) that influence K_T, are shown in Figure 3. Averaged over the 21 sites for the corresponding period, high values of both CA and RH are observed from June to September (Figure 3a,b), whereas higher AOD appears from March to June (Figure 3c). Considering the temporal variations in K_T and the meteorological variables, the seasons with relatively high K_T are characterized by more frequent clear skies due to a dominant high-pressure system in autumn, and strong northerly winds from the continent in winter. The decrease in K_T during July and August can be explained by the attenuation effects of increased cloud and water vapor (RH) during the rainy season, caused by the "Changma" monsoon system. On the other hand, K_T does not exhibit strong seasonal dependence, as shown in Figure 2. This can be attributed to the proximity of numerous sites to the sea, which further tends to dampen strong seasonal variations in the moisture content of the atmosphere as well as in the distribution of the cloud cover [37,38].

The general pattern of monthly average K_T values over the 21 sites is not the same for all regions, particularly Jeju Island located in the South Sea, southwest of the Korean Peninsula. Minima of 0.29 in January and 0.33 in December/January are observed at Jeju and Gosan, respectively (Table 1). To explain this difference, the monthly distributions of CA, RH, and AOD for the Jeju and Gosan sites are presented in Figure 3d–f. Interestingly, the temporal variations in CA over Jeju Island are quite different to those at other sites (Figure 3a,d), while variations in RH and AOD are similar at all sites. For Jeju and Gosan, a relatively high CA occurs in December and January, indicating a different climate pattern between the mainland and the island. The decrease in K_T over Jeju Island in December and January can be attributed to frequent overcast skies, due to the combined effects of strong northwest prevailing winds in winter and a geographical location adjacent to the sea. These results indicate that the monthly variations in K_T are closely related to variations in cloudiness at the respective sites. The contribution of CA to K_T variations is discussed further in Section 3.4. In addition, Ogunjobi *et al.* [9] analyzed the characteristics of K_T using global solar radiation data for the period 1998–2000 at only two sites, Gwangju and Seoul, with similar results to this study.

Figure 2 also suggests that seasonal variations for both clear ($N < 0.3$) and overcast ($N > 0.7$) skies are much weaker than those for all-sky conditions due to cloudless skies or almost constant cloud effects over the whole year, with respective annual means of 0.63 and 0.25. The K_T values under clear sky conditions range from 0.60 (December) to 0.66 (February), while the K_T values under overcast skies range from 0.24 (December and January) to 0.28 (June). The annual mean K_T of 0.63 for clear skies is consistent with the value of 0.62 for clear days, as reported by Jo and Kang [39] using monthly data at 16 sites in Korea from 1982 to 2005. Previous studies have also used threshold values of K_T to characterize sky conditions: clear sky ($K_T > 0.65$), cloudy sky ($0.35 < K_T < 0.65$), and overcast sky ($K_T < 0.35$) [23,40,41]. While the value of 0.65 for clear sky conditions is comparable to the K_T of 0.63 in this study, the threshold for determining overcast skies ($K_T = 0.35$) is higher than our

data suggest (K_T = 0.25). Classifying overcast sky conditions in Korea may therefore require a more detailed treatment.

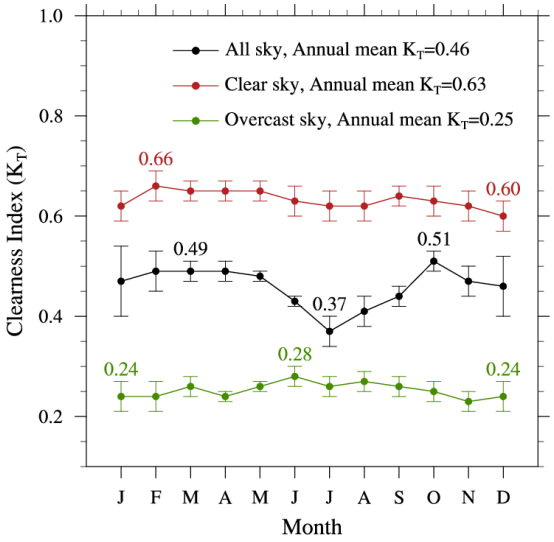

Figure 2. Temporal variations in monthly mean K_T values averaged over all 21 sites. Data are shown for all sky (black circles), clear sky (red circles), and overcast sky (green circles).

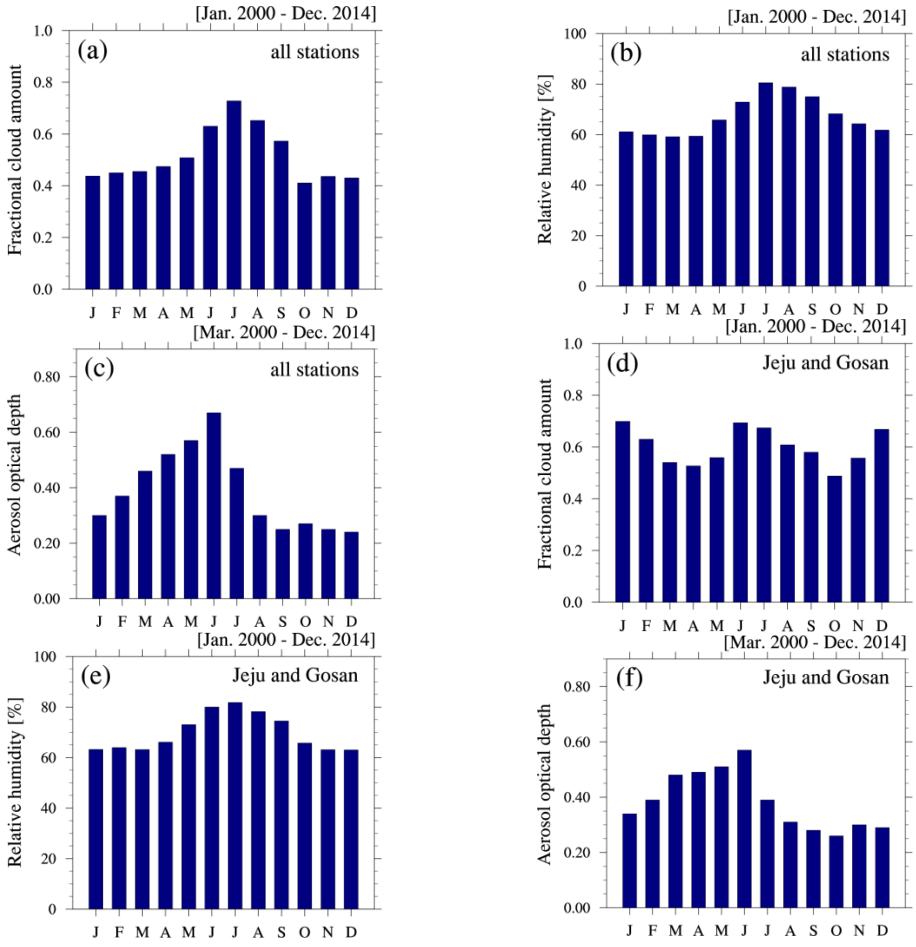

Figure 3. Temporal variations in monthly mean (**a**) CA; (**b**) RH; and (**c**) AOD, averaged over all 21 sites; (**d**–**f**) Same as (**a**–**c**) but for the Jeju and Gosan sites.

Table 1. Monthly climatology of K_T under all-sky conditions at the 21 measurement sites.

Site	January	February	March	April	May	June	July	August	September	October	November	December	Annual
Daegwallyeong	0.56	0.56	0.52	0.49	0.48	0.43	0.36	0.37	0.40	0.50	0.50	0.53	0.48
Chuncheon	0.49	0.51	0.49	0.47	0.48	0.46	0.36	0.41	0.45	0.49	0.45	0.46	0.46
Gangneung	0.55	0.48	0.47	0.48	0.47	0.42	0.37	0.38	0.44	0.50	0.49	0.51	0.46
Seoul	0.44	0.47	0.46	0.45	0.45	0.40	0.30	0.35	0.42	0.48	0.43	0.44	0.42
Incheon	0.47	0.50	0.49	0.47	0.46	0.42	0.34	0.39	0.44	0.49	0.45	0.45	0.45
Wonju	0.48	0.49	0.48	0.47	0.48	0.45	0.36	0.40	0.45	0.50	0.45	0.47	0.46
Suwon	0.49	0.51	0.50	0.48	0.48	0.44	0.35	0.40	0.44	0.51	0.46	0.47	0.46
Seosan	0.48	0.51	0.50	0.49	0.48	0.43	0.35	0.41	0.45	0.50	0.45	0.45	0.46
Cheongju	0.47	0.48	0.49	0.48	0.48	0.43	0.35	0.40	0.44	0.49	0.44	0.44	0.45
Daejeon	0.49	0.52	0.51	0.51	0.51	0.45	0.37	0.42	0.46	0.53	0.48	0.47	0.48
Chupungnyeong	0.50	0.50	0.50	0.49	0.47	0.42	0.36	0.38	0.42	0.50	0.48	0.48	0.46
Pohang	0.53	0.51	0.50	0.50	0.48	0.44	0.40	0.40	0.41	0.48	0.52	0.54	0.48
Daegu	0.51	0.51	0.51	0.50	0.49	0.43	0.38	0.39	0.43	0.50	0.49	0.51	0.47
Jeonju	0.45	0.46	0.48	0.48	0.47	0.42	0.35	0.39	0.44	0.50	0.45	0.43	0.44
Gwangju	0.47	0.50	0.51	0.50	0.49	0.41	0.36	0.40	0.45	0.53	0.49	0.46	0.46
Busan	0.54	0.52	0.50	0.50	0.48	0.43	0.40	0.43	0.44	0.50	0.52	0.53	0.48
Mokpo	0.45	0.48	0.50	0.50	0.48	0.42	0.39	0.44	0.47	0.53	0.48	0.42	0.46
Heuksando	0.39	0.46	0.52	0.52	0.49	0.43	0.37	0.46	0.49	0.54	0.47	0.39	0.46
Jeju	0.29	0.38	0.45	0.49	0.48	0.42	0.45	0.45	0.44	0.48	0.40	0.30	0.42
Gosan	0.33	0.44	0.49	0.51	0.49	0.41	0.44	0.49	0.50	0.53	0.43	0.33	0.45
Jinju	0.53	0.52	0.52	0.50	0.48	0.41	0.38	0.41	0.45	0.54	0.52	0.54	0.48
AVERAGE	0.47	0.49	0.49	0.49	0.48	0.43	0.37	0.41	0.44	0.51	0.47	0.46	0.46

3.2. Spatial Distributions

The nationwide spatial distributions of annual and monthly K_T climatology are shown in Figure 4a–c for the whole year, January (representing winter), and July (representing summer), respectively. In Figure 4a, the spatial distribution of annual climatology shows the highest K_T values in the southeastern region covering five sites (Daegwallyeong, Daejeon, Jinju, Pohang, and Busan), with a total annual mean K_T of 0.48. Lower K_T values are found in the mid-west region covering the Seoul, Incheon, and Jeonju sites, and in the Jeju Island region that includes the Jeju and Gosan sites; these values are in the range of 0.42–0.45 with a minimum value of 0.42 at Seoul and Jeju. These relative regional differences can be attributed to local climate and environmental characteristics, as noted for the temporal variations. The annual climatology of AOD (0.52) for the period of 2000–2014 in Seoul and Incheon, covering the largest metropolitan area in Korea, is higher by 33% than that recorded at other sites (0.39). This result may reflect that the sky conditions at these two sites are relatively turbid, resulting in lower K_T values due to enhanced attenuation effects. In Jeju and Gosan, the regional climate pattern shows a high frequency of cloud formation that may lead to lower K_T values; the annual climatology of CA (6.02) at these two sites is 17% higher than that of other sites (5.14).

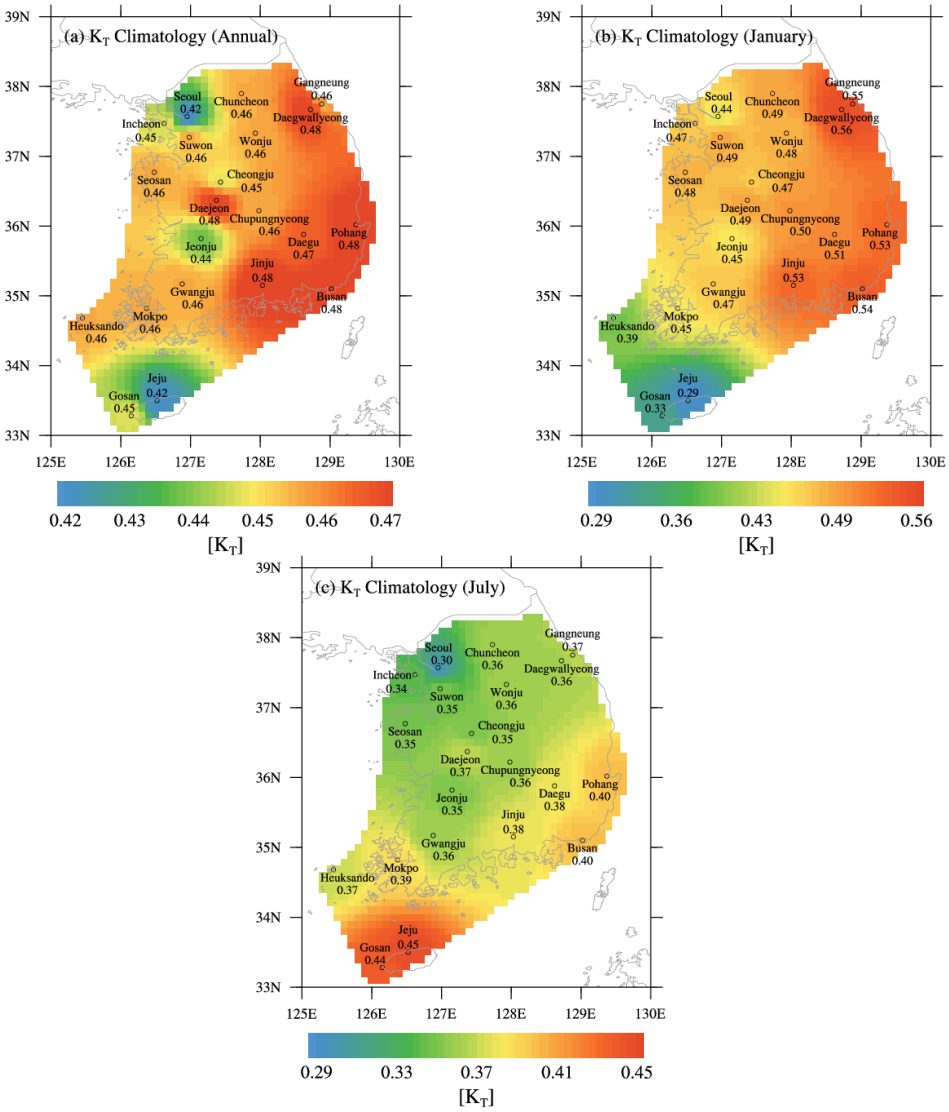

Figure 4. Spatial distributions of K_T climatology in Korea: (**a**) annual; (**b**) January; and (**c**) July.

As shown in Figure 4b, the spatial distribution of January K_T climatology is similar to the annual pattern. High K_T values in the range of 0.51–0.56 appear in the eastern and southeastern regions covering the Daegwallyeong, Gangneung, Pohang, Daegu, Busan, and Jinju sites, whereas low K_T values in the range of 0.29–0.45 are observed in the mid-west region covering the Seoul, Jeonju, and Mokpo sites and the southwest islands (*i.e.*, Jeju, Gosan, and Heuksando). Of note, the sites with higher K_T values in Figure 4a,b are located in eastern (*i.e.*, the Yeongdong district) and southeastern (*i.e.*, the Yeongnam district) regions of the Taebaek Mountains that stretch longitudinally along the eastern edge of the Korean Peninsula. This is the leeward side of the peninsula, which is characterized by clearer and drier conditions, which may result in higher atmospheric transmission of radiation. The spatial distribution of K_T climatology in July (Figure 4c) is dissimilar to the annual and winter patterns. Higher K_T values appear in the Jeju Island regions (Jeju and Gosan), while lower values are found in the northern region covering the Seoul, Incheon, Suwon, Seosan, and Cheongju sites, within the range of 0.30–0.35. The spatial pattern of K_T climatology in July, which gradually increases from north to south, is different from that found in January. In addition, the K_T minimum–maximum range for summer is lower than that for winter. These differences may be related to varying weather patterns between the winter and summer seasons, which are characterized by prevailing northwesterly and southeasterly winds, respectively. Based on the evident relationship between spatio-temporal distributions of K_T and the changes of atmospheric compositions, the continuous monitoring of K_T is necessary in determining the potential of solar power utilization in Korea.

3.3. Long-Term Trends

A simple linear regression analysis of K_T values was performed to evaluate long-term trends, using the slope of the linear regression fit, from the time series of deseasonalized monthly mean K_T values for the 15 years from 2000 to 2014. The deseasonalized values were calculated with respect to climatological monthly means for the 15-year period. A similar method was used to analyze the long-term trends in CA, RH, and AOD. While the trends of K_T, CA, and RH show regional differences, the relative values for the slope of the fit line averaged over the 21 sites were 0.65%, 1.24%, and 1.48% per decade, respectively, suggesting general increases in Korea. However, the AOD trend shows an overall decrease for all sites of less than −13% per decade at the Seosan, Daegu, Jeonju, and Jinju sites.

Table 2 summarizes trends in K_T, CA, RH, and AOD for two sets of measurement sites: those for which K_T is increasing (termed "brightening") and those for which K_T is decreasing (termed "dimming"). The sites with strongly increasing K_T values (>4% per decade in Table 2) are generally in the middle and the southeastern regions of the Korean Peninsula, and include the Daegwallyeong, Seoul, Daejeon, Daegu, and Jinju sites. The highest positive trend (+8.30% per decade) is found at the Daegu site (Figure 5a). The strong increase in K_T at the Daegu site is caused by the decreasing trends in RH of −3.83% per decade and AOD of −13.79% per decade (Table 2). The sites with strongly decreasing K_T values (<−4% per decade in Table 2) are located in the southwestern regions covering Seosan, Cheonju, and Mokpo, with the strongest negative trend (−6.76% per decade) at the Mokpo site (Figure 5b). The strong decreasing trend in K_T at the Mokpo site can be related to increasing trends in CA of +3.53% per decade and RH of +10.31% per decade even though a decreasing trend in AOD is observed (Table 2).

Overall, the trends in meteorological parameters such as CA, RH, and AOD were difficult to relate to trends in K_T. The variations in K_T may be caused by the combined effects of the three variables, or their contributions influencing K_T may be relatively different. As mentioned above, the Seoul site recorded the lowest annual K_T value (0.42) in Korea, but with a significant brightening trend (+4.08% per decade). In terms of long-term trends, Ohmura and Lang [42] reported that decadal fluctuations in global solar radiation at 24 sites in Europe were attributed to a change in cloud conditions. Liepert *et al.* [43] concluded that variations in global solar radiation in Germany were related mainly to aerosols. Ohmura [44] reported that a 20-year dimming phase from 1960 to 1980 and a 15-year brightening phase from 1990 to 2005 were observed in Europe and Japan, concluding that

these trends were related to variations in the aerosol content of the atmosphere. Considering these previous findings, it can be suggested that the long-term K_T trends depend on temporal and spatial variability of atmospheric properties. In this study, the regional dimming and brightening trends are attributed mainly to the meteorological parameters prevailing over the respective regions.

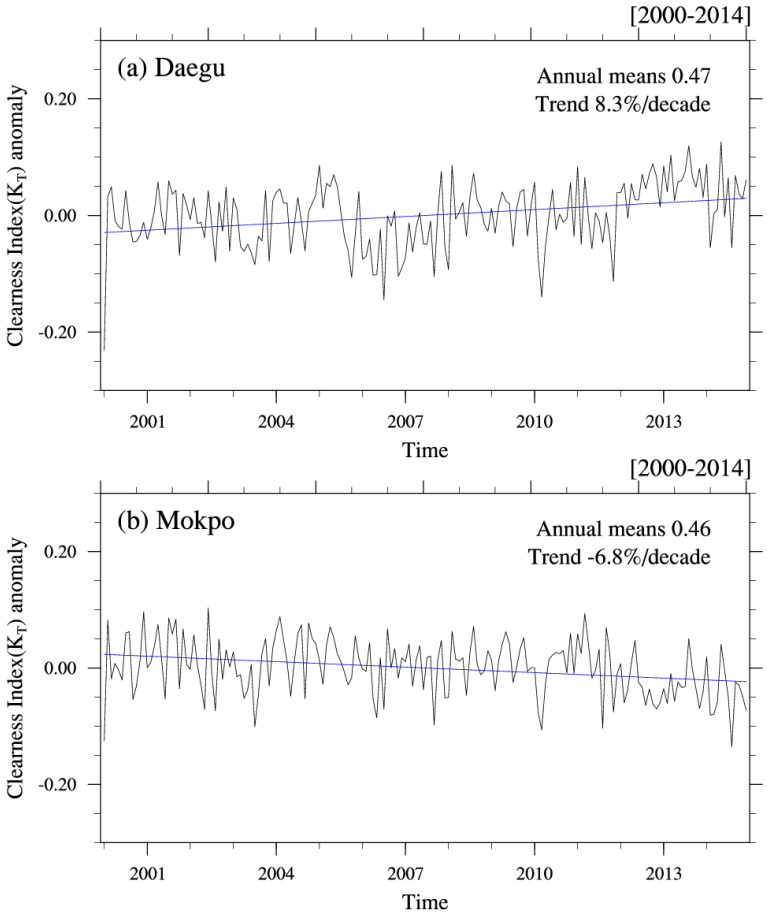

Figure 5. Long-term trend in the deseasonalized K_T anomaly for the (**a**) Daegu and (**b**) Mokpo sites.

Table 2. Long-term trends (Unit: %/decade, 15 years: 2000–2014) in K_T, CA, RH, and AOD at sites in two regions, grouped by increasing and decreasing trends in K_T. The analysis period at the site marked by an asterisk (*) was 7 years (2008–2014).

Increasing K_T Trend (>+4.0%/Decade)				
Site	**K_T**	**CA**	**RH**	**AOD**
Seoul	4.08	−0.18	−3.21	−7.43
Daegwallyeong	4.26	4.35	−1.30	−4.32
Jinju	4.55	0.04	0.88	−13.79
Daejeon	5.57	−1.22	4.03	−9.10
Daegu	8.30	0.94	−3.83	−13.79
Decreasing K_T Trend (<−4.0%/Decade)				
Site	**K_T**	**CA**	**RH**	**AOD**
Cheongju	−4.54	−2.58	−0.11	−9.10
Seosan	−6.25	−6.20	5.35	−13.41
Mokpo	−6.76	3.53	10.31	−11.22
Gangneung *	−10.49	8.82	−7.87	−4.32

3.4. Contributions of CA, RH, and AOD to K_T Variations

To determine the respective contributions of CA, RH, and AOD to K_T, multiple linear regression analyses of the three variables with respect to K_T were performed using daily mean data measured at each of the 21 sites. The partial correlation coefficients of CA, RH, and AOD with K_T are given in Table 3. K_T is negatively correlated with CA, RH, and AOD, and the mean values of partial correlation coefficients averaged over all sites are −0.72 (range, −0.66 to −0.80), −0.45 (−0.13 to −0.58), and −0.37 (−0.19 to −0.49), respectively (Table 3). This result suggests that all three variables significantly affect K_T and that CA is the most influential.

Table 3. Partial correlation coefficients of CA, RH, and AOD with K_T variations, and combined (R^2) and individual contributions to variations in K_T.

Site	R^2	Partial Correlation Coefficients (γ_{1n})			Individual Contribution (%)		
		γ_{12} (CA)	γ_{13} (RH)	γ_{14} (AOD)	CA	RH	AOD
Daegwallyeong	0.59	−0.75	−0.56	−0.31	47.1	9.0	2.8
Chuncheon	0.57	−0.71	−0.48	−0.45	36.6	11.1	9.7
Gangneung	0.64	−0.80	−0.55	−0.36	57.3	3.7	3.4
Seoul	0.60	−0.71	−0.58	−0.41	36.4	16.5	6.8
Incheon	0.47	−0.66	−0.43	−0.39	35.3	6.2	5.8
Wonju	0.58	−0.71	−0.46	−0.43	39.3	10.1	8.2
Suwon	0.54	−0.69	−0.50	−0.37	36.6	12.7	4.9
Seosan	0.60	−0.69	−0.52	−0.43	35.1	15.8	8.6
Cheongju	0.51	−0.66	−0.49	−0.36	31.7	13.3	6.4
Daejeon	0.59	−0.72	−0.43	−0.42	41.5	9.2	8.6
Chupungnyeong	0.59	−0.73	−0.48	−0.39	41.5	10.2	7.6
Pohang	0.56	−0.72	−0.52	−0.39	42.3	7.6	6.0
Daegu	0.53	−0.67	−0.52	−0.44	30.3	13.7	9.4
Jeonju	0.59	−0.71	−0.48	−0.36	39.4	13.1	6.4
Gwangju	0.59	−0.71	−0.53	−0.34	39.4	14.3	5.2
Busan	0.55	−0.72	−0.45	−0.41	44.4	4.4	6.2
Mokpo	0.54	−0.69	−0.41	−0.31	41.6	8.5	4.3
Heuksando	0.61	−0.76	−0.28	−0.35	54.8	0.4	5.6
Jeju	0.63	−0.79	−0.26	−0.19	63.3	−1.0	0.7
Gosan	0.55	−0.73	−0.13	−0.26	53.9	−1.2	2.4
Jinju	0.55	−0.69	−0.41	−0.49	36.9	6.5	12.1
Average	0.57	−0.72	−0.45	−0.37	42.1	8.8	6.2

Cho *et al.* [30] developed a multiple regression model to evaluate the effects of three variables on downward longwave radiation using daily temperature, specific humidity, and cloud amount at King Sejong Station, Antarctica. Similarly, in this study we have developed multiple regression models to evaluate the individual contributions of clouds, water vapor, and aerosols to K_T variations for the 15 years from 2000 to 2014, using the coefficients of partial correlation (r) and the beta coefficients (β) from the statistical equation, $R^2 = \beta_1 r_{11} + \beta_2 r_{12} + \beta_3 r_{13} + \beta_4 r_{14}$ (*cf.* [45]). Table 3 presents the total and individual contributions of the three variables to K_T variations. The multiple regression models show that, on average, CA, RH, and AOD together explained 57.1% (R^2 = 0.57) of the K_T variations under all-sky conditions. Of the total contribution of 57.1%, the individual contributions of CA, RH, and AOD are 42.1%, 8.8%, and 6.2%, respectively. Thus, the cloud effect was the dominant contributor, and the aerosol effect was the least important in explaining K_T variations in Korea.

4. Summary and Conclusions

This study examined seasonal variations in, and the spatial distribution of, the clearness index (K_T) using ground-based measurements of global solar irradiance for the 15-year period of 2000–2014 at 21 sites in Korea. The annual mean K_T value averaged over all sites was 0.46, with values of 0.63

and 0.25 for clear and overcast skies, respectively. A monthly minimum value for K_T of 0.37 occurred in July at all sites except for Jeju, where the minimum occurred in January (K_T = 0.29), and Gosan, where the minimum occurred in December/January (K_T = 0.33). The relatively low K_T values in July were attributed mainly to enhanced attenuation effects by increased water vapor and clouds during the rainy season, which is caused by the "Changma" monsoon system. The low K_T values over Jeju Island in December and January can be attributed to frequent cloudy conditions due to the strong northwest prevailing winds in winter and a geographical location surrounded by the sea. The monthly maximum K_T value was 0.51 in October, with a secondary maximum of 0.49 in February, March, and April. The highest annual K_T value was 0.48, as recorded at the Daegwallyeong, Daejeon, Jinju, Pohang, and Busan sites, all of which are in the southeastern region. The lowest K_T value of 0.42 was found at the Seoul site, but showed an increasing long-term trend. The highest positive trends in K_T (>+4% per decade) occurred in the middle and southeastern regions, with the largest brightening trend of +8.30% per decade occurring at the Daegu site. The largest negative trends in K_T (<−4% per decade) were recorded in the southwestern regions and the largest dimming trend of −6.76% per decade was recorded at the Mokpo site. Multiple linear regression models for K_T using daily data for cloud amount, relative humidity, and aerosol optical depth were developed to evaluate their contributions to K_T variations. The three variables together explain 57% of the variance in daily mean K_T, of which 42% is explained by cloudiness, 9% by relative humidity, and 6% by aerosol optical depth. Thus, the K_T variations were affected mainly by clouds with relatively weak aerosol effects in Korea, despite heavy aerosol loading throughout the year. This finding may indicate an indirect effect of aerosol particles on cloud microphysics. However, an evaluation of the indirect aerosol effects on clouds, and thus K_T, would require a detailed investigation using comprehensive models and a diverse measurement dataset.

Acknowledgments: This work was funded by "Geostationary Environment Monitoring Spectrometer (GEMS) Program (2012000160002)" of the Korea Ministry of Environment and the Korea Meteorological Administration Research and Development Program under Grant KMIPA 2015-5170. The authors acknowledge Hi Ku Cho for invaluable suggestions.

Author Contributions: Yeonjin Jung, Jaemin Kim, and Yun Gon Lee conceived and designed this research; Hana Lee, Jaemin Kim, and Youngbum Cho analyzed the data and provided main materials of this paper; Yeonjin Jung and Yun Gon Lee wrote the paper.

Conflicts of Interest: The authors declare no conflict of interest.

References

1. Che, H.; Shi, G.; Zhang, X.; Arimoto, R.; Zhao, J.; Xu, L.; Wang, B.; Chen, Z. Analysis of 40 years of solar radiation data from China, 1961–2000. *Geophys. Res. Lett.* **2005**, *32*. [CrossRef]
2. Okogbue, E.; Adedokun, J.; Holmgren, B. Hourly and daily clearness index and diffuse fraction at a tropical station, Ile-Ife, Nigeria. *Int. J. Climatol.* **2009**, *29*, 1035–1047. [CrossRef]
3. Bano, T.; Singh, S.; Gupta, N.; John, T. Solar global ultraviolet and broadband global radiant fluxes and their relationships with aerosol optical depth at New Delhi. *Int. J. Climatol.* **2013**, *33*, 1551–1562. [CrossRef]
4. Liu, B.Y.; Jordan, R.C. The interrelationship and characteristic distribution of direct, diffuse and total solar radiation. *Sol. Energy* **1960**, *4*, 1–19. [CrossRef]
5. Iqbal, M. *An Introduction to Solar Radiation*; Academic Press: San Diego, CA, USA, 1983; p. 390.
6. Ideriah, F.; Suleman, S. Sky conditions at Ibadan during 1975–1980. *Sol. Energy* **1989**, *43*, 325–330. [CrossRef]
7. Elhadidy, M.; Abdel-Nabi, D.; Kruss, P. Ultraviolet solar radiation at Dhahran, Saudi Arabia. *Sol. Energy* **1990**, *44*, 315–319. [CrossRef]
8. Udo, S. Sky conditions at Ilorin as characterized by clearness index and relative sunshine. *Sol. Energy* **2000**, *69*, 45–53. [CrossRef]
9. Ogunjobi, K.; Kim, Y.; Adedokun, J.; Ryu, S.; Kim, J. Analysis of sky condition using solar radiation data at Kwangju and Seoul, South Korea and Ile-Ife, Nigeria. *Theor. Appl. Climatol.* **2002**, *72*, 265–272. [CrossRef]
10. Foyo-Moreno, I.; Vida, J.; Alados-Arboledas, L. A simple all weather model to estimate ultraviolet solar radiation (290–385 nm). *J. Appl. Meteorol.* **1999**, *38*, 1020–1026. [CrossRef]

11. Cañada, J.; Pedrós, G.; López, A.; Boscá, J. Influences of the clearness index for the whole spectrum and of the relative optical air mass on UV solar irradiance for two locations in the Mediterranean area, Valencia and Cordoba. *J. Geophys. Res.* **2000**, *105*, 4759–4766. [CrossRef]
12. Adam, M. Atmospheric modulations of the ratio of UVB to broadband solar radiation: Effect of ozone, water vapour, and aerosols at Qena, Egypt. *Int. J. Climatol.* **2014**, *34*, 2477–2488. [CrossRef]
13. Adam, M.E.-N. Determination of daily total ultraviolet-B in a subtropical region (Upper Egypt): An empirical approach. *Atmos. Res.* **2015**, *153*, 1–9. [CrossRef]
14. Wang, L.; Gong, W.; Lin, A.; Hu, B. Measurements and cloudiness influence on UV radiation in Central China. *Int. J. Climatol.* **2014**, *34*, 3417–3425. [CrossRef]
15. Wang, L.; Gong, W.; Luo, M.; Wang, W.; Hu, B.; Zhang, M. Comparison of different UV models for cloud effect study. *Energy* **2015**, *80*, 695–705. [CrossRef]
16. Alados-Arboledas, L.; Alados, I.; Foyo-Moreno, I.; Olmo, F.; Alcántara, A. The influence of clouds on surface UV erythemal irradiance. *Atmos. Res.* **2003**, *66*, 273–290. [CrossRef]
17. Foyo-Moreno, I.; Alados, I.; Alados-Arboledas, L. Adaptation of an empirical model for erythemal ultraviolet irradiance. *Ann. Geophys.* **2007**, *25*, 1499–1508. [CrossRef]
18. Antón, M.; Serrano, A.; Cancillo, M.; García, J. Relationship between erythemal irradiance and total solar irradiance in South-Western Spain. *J. Geophys. Res.* **2008**, *113*. [CrossRef]
19. Antón, M.; Serrano, A.; Cancillo, M.; García, J. An empirical model to estimate ultraviolet erythemal transmissivity. *Ann. Geophys.* **2009**, *27*, 1387–1398. [CrossRef]
20. Udo, S.; Aro, T. Global PAR related to global solar radiation for central Nigeria. *Agric. For. Meteorol.* **1999**, *97*, 21–31. [CrossRef]
21. Wang, L.; Gong, W.; Ma, Y.; Hu, B.; Zhang, M. Photosynthetically active radiation and its relationship with global solar radiation in Central China. *Int. J. Biometeorol.* **2014**, *58*, 1265–1277. [CrossRef] [PubMed]
22. Wang, L.; Gong, W.; Li, C.; Lin, A.; Hu, B.; Ma, Y. Measurement and estimation of photosynthetically active radiation from 1961 to 2011 in Central China. *Appl. Energy* **2013**, *111*, 1010–1017. [CrossRef]
23. Escobedo, J.F.; Gomes, E.N.; Oliveira, A.P.; Soares, J. Modeling hourly and daily fractions of UV, PAR and NIR to global solar radiation under various sky conditions at Botucatu, Brazil. *Appl. Energy* **2009**, *86*, 299–309. [CrossRef]
24. Wang, L.; Gong, W.; Li, J.; Ma, Y.; Hu, B. Empirical studies of cloud effects on ultraviolet radiation in Central China. *Int. J. Climatol.* **2014**, *34*, 2218–2228. [CrossRef]
25. Adam, M.E.-N.; Ahmed, E.A. Comparative analysis of cloud effects on ultraviolet-B and broadband solar radiation: Dependence on cloud amount and solar zenith angle. *Atmos. Res.* **2016**, *168*, 149–157. [CrossRef]
26. Ogunjobi, K.; Kim, Y. Ultraviolet (0.280–0.400 μm) and broadband solar hourly radiation at Kwangju, South Korea: Analysis of their correlation with aerosol optical depth and clearness index. *Atmos. Res.* **2004**, *71*, 193–214. [CrossRef]
27. Adam, M.E.-N. Sensitivity analysis of aerosols' effect in UVB transmission to solar zenith angle at subtropical location (Qena, Egypt). *Atmos. Environ.* **2013**, *71*, 311–318. [CrossRef]
28. Dervishi, S.; Mahdavi, A. Computing diffuse fraction of global horizontal solar radiation: A model comparison. *Sol. Energy* **2012**, *86*, 1796–1802. [CrossRef]
29. Duzen, H.; Aydin, H. Sunshine-based estimation of global solar radiation on horizontal surface at Lake Van region (Turkey). *Energy Convers. Manag.* **2012**, *58*, 35–46. [CrossRef]
30. Cho, H.K.; Kim, J.; Jung, Y.; Lee, Y.G.; Lee, B.Y. Recent changes in downward longwave radiation at King Sejong Station, Antarctica. *J. Clim.* **2008**, *21*, 5764–5776. [CrossRef]
31. Geiger, M.; Diabaté, L.; Ménard, L.; Wald, L. A web service for controlling the quality of measurements of global solar irradiation. *Sol. Energy* **2002**, *73*, 475–480. [CrossRef]
32. Estupiñán, J.G.; Raman, S.; Crescenti, G.H.; Streicher, J.J.; Barnard, W.F. Effects of clouds and haze on UV-B radiation. *J. Geophys. Res.* **1996**, *101*, 16807–16816. [CrossRef]
33. Spitters, C.; Toussaint, H.; Goudriaan, J. Separating the diffuse and direct component of global radiation and its implications for modeling canopy photosynthesis Part I. Components of incoming radiation. *Agric. For. Meteorol.* **1986**, *38*, 217–229. [CrossRef]
34. Jacovides, C.; Tymvios, F.; Assimakopoulos, V.; Kaltsounides, N. The dependence of global and diffuse PAR radiation components on sky conditions at Athens, Greece. *Agric. For. Meteorol.* **2007**, *143*, 277–287. [CrossRef]

35. Duffie, J.A.; Beckman, W.A. *Solar Engineering of Thermal Processes*, 4th ed.; John Wiley & Sons Inc.: Hoboken, NJ, USA, 1980.
36. Cooper, P. The absorption of radiation in solar stills. *Sol. Energy* **1969**, *12*, 333–346. [CrossRef]
37. Erbs, D.; Klein, S.; Duffie, J. Estimation of the diffuse radiation fraction for hourly, daily and monthly-average global radiation. *Sol. Energy* **1982**, *28*, 293–302. [CrossRef]
38. Jacovides, C.; Hadjioannou, L.; Pashiardis, S.; Stefanou, L. On the diffuse fraction of daily and monthly global radiation for the island of Cyprus. *Sol. Energy* **1996**, *56*, 565–572. [CrossRef]
39. Jo, D.-K.; Kang, Y.-H. A study on the analysis of global dimming appearances using the solar radiation measurement in Korean major cities (focused on atmospheric clearness analysis). *J. Korean Sol. Energy Soc.* **2007**, *27*, 45–52.
40. Igawa, N.; Koga, Y.; Matsuzawa, T.; Nakamura, H. Models of sky radiance distribution and sky luminance distribution. *Sol. Energy* **2004**, *77*, 137–157. [CrossRef]
41. Wang, L.; Gong, W.; Ma, Y.; Hu, B.; Wang, W.; Zhang, M. Analysis of ultraviolet radiation in Central China from observation and estimation. *Energy* **2013**, *59*, 764–774. [CrossRef]
42. Ohmura, A.; Lang, H. Secular variation of global radiation in Europe. In Proceedings of the 1989 International Radiation Symposium, Lille, France, 18–24 August 1989; pp. 298–301.
43. Liepert, B. Solar radiation in Germany: Observed trends and their causes. In Proceedings of the 1994 A & WMA International Specialty Conference on Climate Change, Phoenix, AZ, USA, 5–8 April 1994; Air and Waste Management Association: Pittsburgh, PA, USA, 1994.
44. Ohmura, A. Observed decadal variations in surface solar radiation and their causes. *J. Geophys. Res.* **2009**, *114*, D00D05. [CrossRef]
45. Overall, J.E. *Applied Multivariate Analysis*; McGraw-Hill: New York, NY, USA, 1972.